MDPI

Proceeding Paper

Assessment of Cloud-Aerosol Lidar with Orthogonal Polarization–Cloud-Aerosol Lidar and Infrared Pathfinder Satellite Observations Retrievals towards Estimating the Aerosol Direct Impact on the Shortwave Radiation Budgets in North Africa, Europe, and the Middle East [†]

Anna Moustaka [1,2,*], Marios-Bruno Korras-Carraca [1,3], Kyriakoula Papachristopoulou [1,4], Ilias Fountoulakis [1,5], Stelios Kazadzis [6], Emmanouil Proestakis [1], Vassilis Amiridis [1], Kleareti Tourpali [4] and Antonis Gkikas [1,5]

1 Institute for Astronomy, Astrophysics, Space Applications and Remote Sensing, National Observatory of Athens, 11810 Athens, Greece; koras@env.aegean.gr (M.-B.K.-C.); kpapachr@noa.gr (K.P.); i.fountoulakis@noa.gr (I.F.); proestakis@noa.gr (E.P.); vamoir@noa.gr (V.A.); agkikas@noa.gr (A.G.)
2 Department of Physics, Aristotle University of Thessaloniki, 54124 Thessaloniki, Greece
3 Laboratory of Meteorology & Climatology, Department of Physics, University of Ioannina, 45110 Ioannina, Greece
4 Laboratory of Climatology and Atmospheric Environment, Department of Geology and Environment, National and Kapodistrian University of Athens (LACAE/NKUA), 10679 Athens, Greece; tourpali@auth.gr
5 Research Centre for Atmospheric Physics and Climatology, Academy of Athens, 10679 Athens, Greece
6 Physicalisch Meteorologisches Observatorium, 7260 Davos, Switzerland; stelios.kazadzis@pmodwrc.ch
* Correspondence: annamstk@noa.gr
† Presented at the 16th International Conference on Meteorology, Climatology and Atmospheric Physics—COMECAP 2023, Athens, Greece, 25–29 September 2023.

Abstract: The overarching objective of the present study is to assess the quality of the CALIOP–CALIPSO aerosol retrievals towards understanding their advantages and deficiencies. Such analysis is a prerequisite prior to their utilization in a radiation transfer model (RMT) for estimating the clear-sky shortwave (SW) aerosol-induced direct radiative effects (DREs) within the Earth–Atmosphere system. The study region encompasses North Africa, the Middle East, and Europe (NAMEE domain), and the period of interest ranges from 2007 to 2020. A holistic approach has been adopted involving spaceborne retrievals (CALIOP–CALIPSO and MODIS-Aqua) and ground-based measurements (AERONET). Overall, CALIOP underestimates columnar aerosol optical depth (AOD), particularly in dust-rich areas, attributed to various factors (e.g., lidar ratio). In order to demonstrate the significance of an appropriate definition of the lidar ratio, focusing on DREs, three example dust cases are investigated. The CALIPSO dust extinction coefficient profiles are used as inputs to the libRadtran Radiative Transfer Model (RTM) along with other crucial parameters. For each study case, two RTM runs are performed using the default (CALIPSO) and an updated (DeliAn) dust lidar ratio. Our results indicate remarkable differences (up to ~22%) on the surface and atmospheric DREs while varying from 17% to 27% at TOA.

Keywords: CALIOP–CALIPSO; aerosol-radiation interactions; RTM; SW; DREs; NAMEE; MODIS-Aqua; AERONET

1. Introduction

Atmospheric aerosols through their direct and indirect interactions with incoming shortwave (SW) and outgoing longwave (LW) radiation perturb the radiation budget of the Earth–Atmosphere system, subsequently affecting atmospheric processes across various spatiotemporal scales [1]. The present-day estimates of the SW direct radiative effects (DREs), resolved by the current state-of-the-art climate models, show that aerosols,

at a global scale and over long-term periods, tend to cool the Earth–Atmosphere system, partly counterbalancing the induced planetary warming by the greenhouse gases (GHGs). However, global climate models continue to give diverging results regarding the DRE magnitude.

Since June 2006, the Cloud-Aerosol Lidar with Orthogonal Polarization (CALIOP) on board the Cloud-Aerosol Lidar and Infrared Pathfinder Satellite Observations (CALIPSO) satellite has provided a new perception of aerosols and cloud observations [2]. CALIOP (version 4.2) Level 2 aerosol classification scheme utilizes Level-1-layer-intergrated values of depolarization and attenuated backscatter along with ancillary information about the geographical location, the surface type, and layer altitude in order to assign aerosol types [3]. CALIPSO vertically resolved aerosol observations can be utilized for the assessment of aerosol–radiation interactions, acknowledging that, among the factors determining DREs and assuming clear-sky conditions, the aerosols' load, type, vertical structure, and optical properties are the most crucial. However, previous evaluation studies have demonstrated inherent deficiencies that should be defined and addressed prior to a robust estimation of aerosol-speciated DREs.

2. Data and Methodology

Aerosol retrievals. For the purposes of this study, we processed the quality-assured (QA) CALIPSO Level 2 (L2) Version 4.2 (V4) vertically resolved retrievals extracted from the LIVAS database [4]. A series of quality controls was applied ensuring the mitigation of the negative impact on aerosol retrievals due to (i) layer misdetection and misclassification, (ii) extinction retrieval errors, and (iii) biases caused by the negative signal anomaly. In addition, the possible cloud contamination has been minimized relying on the CAD score and the misclassified cirrus fringe filters [5]. AERONET observations of AOD, single scattering albedo (SSA), asymmetry factor (ASYM), and Ångström exponent (AE) were also exploited for the purposes of this study. For the collocation, CALIPSO retrievals residing within a circle, centered at the AERONET site, of a 100 km radius were spatially averaged, whereas AERONET observations within a ±30 min time window, centered at the CALIPSO overpass, were temporally averaged.

Radiative transfer model. For the Radiative Transfer (RT) simulations, in the SW spectral range (280–3000 nm), the UVSPEC model from the libRadtran radiative transfer package [6] has been used. The RTM inputs consisted of the columnar AOD, the vertical profiles of the extinction coefficient at 532nm, along with intensive aerosol optical properties (i.e., single scattering albedo, asymmetry parameter, and Ångström exponent) extracted from the AERONET almucantar retrievals, after collocating ground-based and spaceborne (CALIPSO) observations. Additional parameters such as the surface albedo, ozone, and water vapor columnar concentrations were all extracted from the MERRA-2 reanalysis.

Region of Interest. The region of interest (ROI) consisted of North Africa, the Middle East, and Europe (NAMEE domain). Within the geographical limits of the ROI, a variety of aerosol species of natural and anthropogenic origins were encountered (Figure 1).

As a first step, we calculated the frequency of occurrence (expressed in percentages) of each aerosol type categorized based on the CALIPSO classification scheme over the study period (January 2007–December 2020). The obtained results, shown in Figure 1b, were produced by taking into account the QA-filtered retrievals throughout troposphere and stratosphere (up to 30 km). Among the aerosol species in the NAMEE domain, a clear predominance of dust aerosols either when these were solely detected (~52%) or were mixed with pollutants (~18%) and marine particles (~9%) was evident. About 10% of the total sample corresponded to sea salt aerosols, whereas the frequencies for the remaining aerosol species did not exceed 5%.
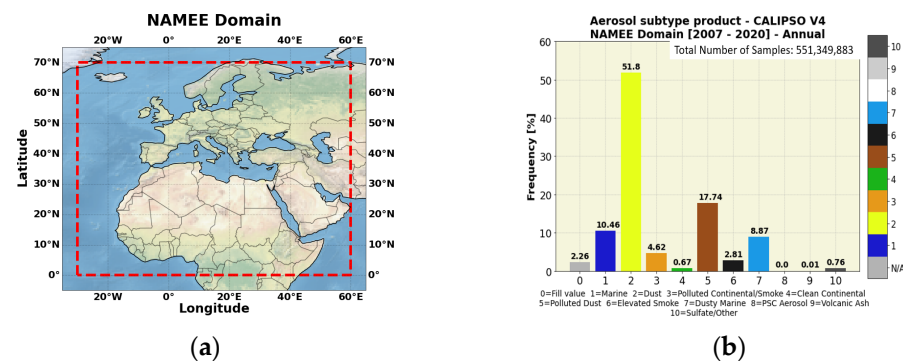
Figure 1. (**a**) Geographical limits of the NAMEE domain and (**b**) frequency of occurrence for each aerosol subtype according to the existing CALIOP V4 classification scheme.

3. Results

Evaluation of the CALIOP–CALIPSO retrievals. Errors in the CALIPSO product can largely be attributed either to the mistyping of aerosol layers or to the incorrect modelling of aerosol microphysics, which can result in large underestimations of the order of 13% in terms of AOD [3]. A significant source of uncertainty arises also from the limitation of CALIPSO to identify tenuous aerosol layers, whereas opaque cloud or aerosol layers significantly attenuate or even block the transmission of the laser beam, making the detection of the underneath layers infeasible.

A comparison of the CALIPSO AOD versus AERONET (Figure 2a) and MODIS-Aqua (Figure 2b) was performed. Overall, CALIPSO tended to underestimate AOD, and the negative biases against AERONET increased as the intensity of aerosol loads increased (Figure 2a). Biases against MODIS were highly distinguishable over the Saharan desert and specifically over well-known dust sources (e.g., Bodélé), an inadequacy strongly related to the presence of opaque dust layers completely attenuating the laser beam. Above seas, the negative CALIPSO-MODIS declinations were found in downwind dust regions. Slightly positive and negative differences were recorded in Central and Northern Europe, respectively.
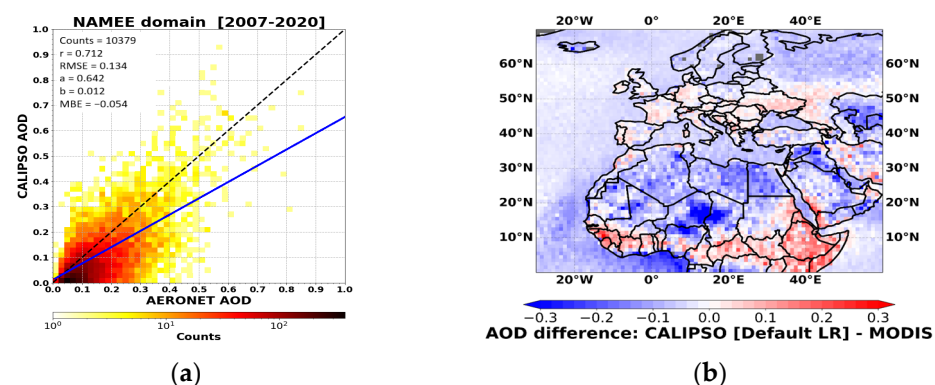
Figure 2. Comparison of CALIPSO AOD with (**a**) AERONET (the blue line shows the linear regression, while the black one-to-one dashed line correspond to no AOD difference between AERONET and CALIPSO) and (**b**) MODIS AOD, respectively.

Case studies. For the derivation of the extinction coefficient and the columnar AOD, a Lidar Ratio (LR) is required (i.e., the ratio of extinction to backscatter), which is predefined for each aerosol type classified in the CALIPSO retrieval scheme. In order to examine the validity of the LRs used in CALIOP V4 retrievals, we focused initially on dust cases using in-parallel LRs adapted from the DeLiAn database [7] (Figure 1b). In Figure 3, pure dust layers that extended over El Farafra, Lampedusa, and IER Cinzana are presented. The respective attenuated backscatter at 532 nm was averaged along the orbits, and the

extinction coefficients are calculated with the CALIPSO default LR for dust (44 sr) (red line) and the revised from the DeLiAn database (53 sr) (green line). For the computation of AOD, the extinction coefficient at 532nm was integrated for both LRs, and the results were compared with the respective AERONET AODs temporally averaged for different time windows (± 15, ± 30, ± 45, and ± 60 min, with respect to the satellite overpass). Thanks to the utilization of the revised dust LR, the bias against AERONET AODs was reduced by ~20%.
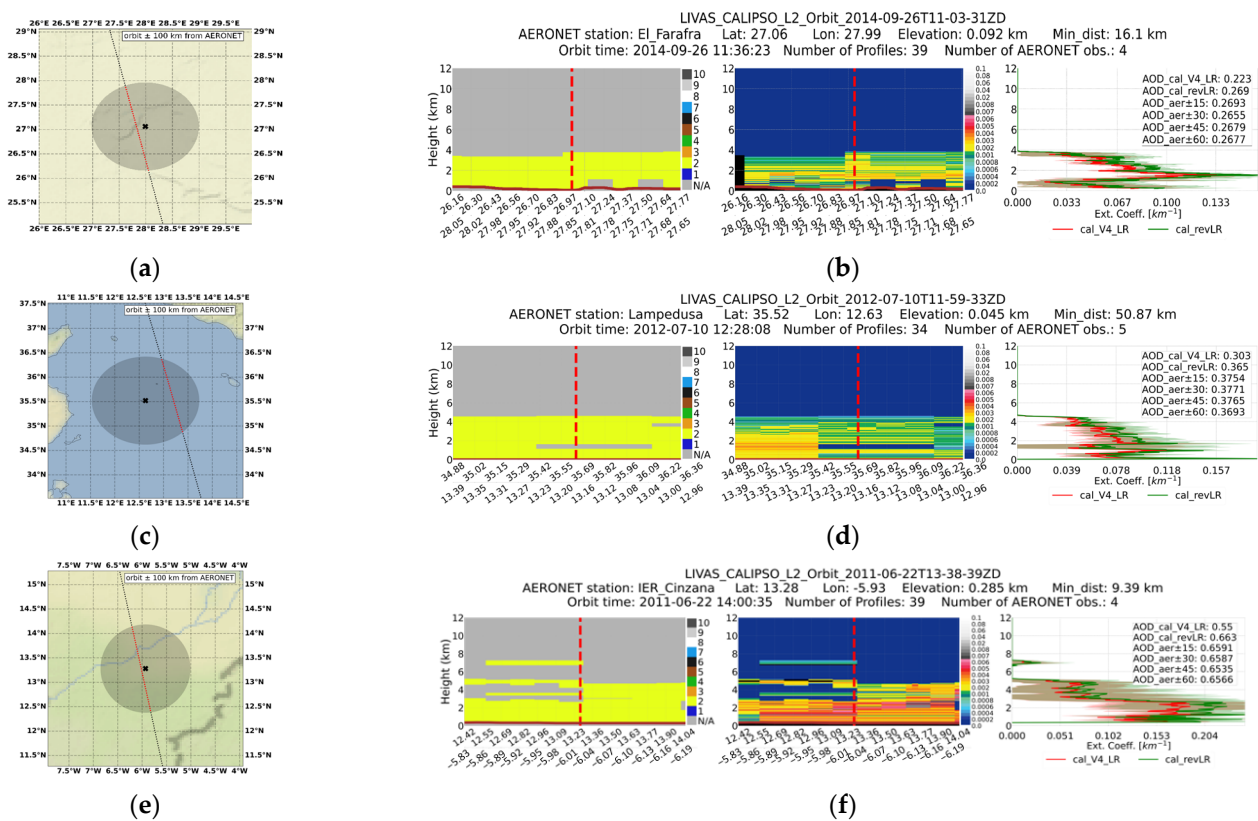
Figure 3. CALIPSO overpass from (**a**) El_Farafra, (**c**) Lampedusa, (**e**) IER_Cinzana stations, and (**b**,**d**,**f**) the respective observations of V4 aerosol subtype product, the total attenuated backscatter coefficient 532 nm, and the extinction coefficient 532 nm, along with the corresponding AOD.

RTM analysis. For all cases, we calculated the clear-sky shortwave direct radiative effects (DREs) (using the input parameters from Table 1) at the top of the atmosphere (TOA), within the atmosphere (ATM) and at the Earth's surface (NETSRFC) based on the following equations.

$$\mathrm{DRE_i = F_{NET,i}^{RADON} - F_{NET,i}^{RADOFF}} \ (1), \ \mathrm{DRE_{ATM} = DRE_{TOA} - DRE_{NETSRFC}} \ (2), \ i = TOA, ATM, SRFC$$

Table 1. UVSPEC model input parameters.

Station	SZA	AOD [532]	SSA	ASYM	AE [440–870]	TCWV [mm/cm²]	TCO [DU]	ALBEDO
El_Farafra	36.75	0.223/0.269 *	0.94	0.72	0.15	20.46	272.96	0.30
Lampedusa	20.82	0.303/0.365	0.94	0.72	0.14	23.32	285.82	0.07
IER_Cinzana	24.66	0.550/0.663	0.94	0.72	0.12	44.39	280.61	0.15

* V4LR/revLR.

The $\mathrm{F_{NET,i}^{RADON}}$ and $\mathrm{F_{NET,i}^{RADOFF}}$ terms represent the radiative fluxes with and without aerosols, respectively. According to Figure 4, dust aerosols cause a large surface cooling

and an atmospheric heating effect. These effects are strongest ($DRE_{SURFNET}$ down to -84.8 W/m^2 and DRE_{ATM} up to 72.6 W/m^2) at the station of IER Cinzana, where the AOD takes its maximum values. Moreover, the $DRE_{NETSRFC}$ is more pronounced in Lampedusa compared to El Farafra, due to the presence of higher aerosol loads. However, the DRE_{ATM} takes similar values in these two stations because the surface albedo is higher compared to Lampedusa in the case of El Farafra, resulting in an increase in the reflected solar radiation at the ground, thus increasing the atmospheric absorption.
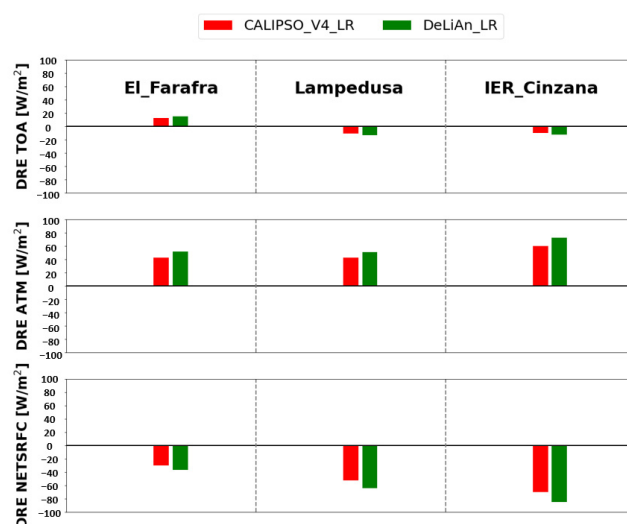
Figure 4. Dust DREs at the top of the atmosphere (TOA), in the atmosphere (ATM), and at the surface (SRFC) over El_Farafra, Lampedusa, and IER_Cinzana stations, with the green and red colors denoting the different AODs used in RT simulations (red—with CALIPSO default LR; and green—with LR from DeLiAn database).

The role of the underlying surface albedo was crucial for the determination of the sign and the magnitude of the aerosol-induced DRE at TOA (planetary effect). According to our results, dust caused a planetary cooling effect over Lambedusa and IER Cinzana (surface albedo 0.07 and 0.15), whereas the multiple scattering between the relatively absorbing dust particles and the underlying highly reflective surface (surface albedo 0.30) resulted in a planetary warming effect (positive sign of the DRE_{TOA}) over El_Farafra. We also found that the employment of the AOD computed with the revised dust LR (DeLiAn database) in the DRE calculations led to an enhancement of the surface cooling and atmospheric warming effects by up to ~22%. At TOA, both the planetary cooling (at IER Cinzana and Lambedusa) and the planetary warming effect (El Farafra) become stronger (changes of the order of ~17–27%).

4. Conclusions

In the current study, focus was given on the performance of the CALIOP–CALIPSO retrievals in terms of representing aerosol loads in the NAMEE domain over the period of 2007–2020. According to our results, CALIOP underestimated AOD with respect to AERONET sunphotometers, whereas it was revealed via the intercomparison against MODIS-Aqua that the maximum and moderate negative biases were recorded in dust sources and dust downwind areas, respectively. Such deficiencies were expected to affect the estimations of the induced direct radiative effects. Representative case studies for dust layers were examined due to the predominance of this type among other aerosol species. An adaptation of a more realistic dust LR selection scheme improves the level of agreement with ground-based observations. Such corrections, among others, will strengthen the reliability of the estimated aerosol direct radiative effects relying on the synergy of CALIOP–CALIPSO aerosol retrievals and radiative transfer models. For the same case studies, dust DREs at TOA, in the atmosphere and at the SRFC, were computed using the default CALIPSO

dust lidar ratio (44 sr) and the corresponding value from the DeLiAn database (53 sr). As expected, a stronger surface cooling and an atmospheric warming was found (by up to ~22%), whereas the increase in the DRE$_{TOA}$ magnitude in absolute terms varied from 17% to 27%. For a next step, the analysis will be implemented for different aerosol scenes and the simulated radiation fields at TOA, and the surface will be evaluated against satellite (CERES) and ground-based (BSRN and GEBA) observations, respectively.

Author Contributions: Conceptualization, A.M. and A.G.; methodology, A.M., S.K., V.A., K.T. and A.G.; software, A.M.; validation, A.M., M.-B.K.-C., E.P., K.P., I.F., V.A., K.T. and A.G.; writing—original draft preparation, A.M. and M.-B.K.-C.; writing—review and editing, all; funding acquisition, A.G. All authors have read and agreed to the published version of the manuscript.

Data Availability Statement: The LIVAS dust products are available upon request from Vassilis Amiridis (vamoir@noa.gr), Emmanouil Proestakis (proestakis@noa.gr), and/or Eleni Marinou (elmarinou@noa.gr).

Conflicts of Interest: The authors declare no conflict of interest.

References

1. Gkikas, A.; Obiso, V.; Perez Garcia-Pando, C.; Jorba, O.; Hatzianastassiou, N.; Vendrell, L.; Basart, S.; Solomos, S.; Gásso, S.; Baldasano, J.M. Direct radiative effects during intense Mediterranean desert dust outbreaks. *Atmos. Chem. Phys.* **2018**, *18*, 8757–8787. [CrossRef]
2. Winker, D.M.; Pelon, J.; Coakley, J.A., Jr.; Ackerman, S.A.; Charlson, R.J.; Colarco, P.R.; Flamant, P.; Fu, Q.; Hoff, R.M.; Kittaka, C.; et al. The CALIPSO mission: A global 3D view of aerosols and clouds. *Bull. Am. Meteorol. Soc.* **2010**, *91*, 1211–1230. [CrossRef]
3. Kim, M.H.; Omar, A.H.; Tackett, J.L.; Vaughan, M.A.; Winker, D.M.; Trepte, C.R.; Hu, Y.; Liu, Z.; Poole, L.R.; Pitts, M.C.; et al. The CALIPSO version 4 automated aerosol classification and lidar ratio selection algorithm. *Atmos. Meas. Tech.* **2018**, *11*, 6107–6135. [CrossRef] [PubMed]
4. Amiridis, V.; Marinou, E.; Tsekeri, A.; Wandinger, U.; Schwarz, A.; Giannakaki, E.; Mamouri, R.; Kokkalis, P.; Binietoglou, I.; Solomos, S.; et al. LIVAS: A 3-D multi-wavelength aerosol/cloud database based on CALIPSO and EARLINET. *Atmos. Chem. Phys.* **2015**, *15*, 7127–7153. [CrossRef]
5. Tackett, J.L.; Winker, D.M.; Getzewich, B.J.; Vaughan, M.A.; Young, S.A.; Kar, J. CALIPSO lidar level 3 aerosol profile product: Version 3 algorithm design. *Atmos. Meas. Tech.* **2018**, *11*, 4129–4152. [CrossRef] [PubMed]
6. Emde, C.; Buras-Schnell, R.; Kylling, A.; Mayer, B.; Gasteiger, J.; Hamann, U.; Kylling, J.; Richter, B.; Pause, C.; Dowling, T.; et al. The libRadtran software package for radiative transfer calculations (version 2.0.1). *Geosci. Model Dev.* **2016**, *9*, 1647–1672. [CrossRef]
7. Floutsi, A.A.; Baars, H.; Engelmann, R.; Althausen, D.; Ansmann, A.; Bohlmann, S.; Heese, B.; Hofer, J.; Kanitz, T.; Haarig, M.; et al. DeLiAn–a growing collection of depolarization ratio, lidar ratio and Ångström exponent for different aerosol types and mixtures from ground-based lidar observations. *Atmos. Meas. Tech.* **2022**, *16*, 2353–2379. [CrossRef]